9.

Design of Steel Triangular Plate Energy Absorbers for Seismic-Resistant Construction

Keh-Chyuan Tsai, M.EERI, Huan-Wei Chen, Ching-Ping Hong, and Yung-Feng Su

Building structures must be constructed to dissipate a large amount of seismic energy in order to achieve economical earthquake-resistant constructions. In this paper, recent research findings on the effectiveness of using steel triangular plates welded as the added damping and stiffness (ADAS) device for earthquake-resistant structures are presented. Experimental results indicate that a properly welded steel triangular-plate added damping and stiffness device (TADAS) can sustain a large number of yielding reversals without any stiffness or strength degradation. The effects of the ratio of the TADAS element stiffness to that of the bare frame, and the ratio of the entire frame yield strength to that associated with the TADAS element on the seismic response of the added damping and stiffness structures are discussed. Based on these studies, a design methodology and an example are developed for the application of the TADAS device in earthquake-resistant constructions.

INTRODUCTION

In order to achieve economical earthquake-resistant buildings, building structures must be constructed to absorb and dissipate a large amount of seismic energy. In recent years, a number of researchers have investigated techniques of increasing the building energy absorbing capacity through the use of steel-plate added damping and stiffness (ADAS) device (Bergman and Goel 1987, Whittaker et al. 1989, Su and Hanson 1990, Xia and Hanson 1992). These studies have confirmed that the ADAS device using X-shaped steel plates is suitable for buildings to resist earthquake forces. However, as the ADAS devices used in these studies were made of X-shaped steel plates bolted together through two ends of each plate, the stiffness of the device has been found very sensitive to the tightness of the bolts and generally the stiffness obtained is much less than that predicted by assuming both ends are fixed (Whittaker et al. 1989).

Since the bending curvature produced by a transverse force applying at the end of the triangular plate is uniform over the full height of the plate, the plate can deform well into the inelastic range without curvature concentration. The steel triangular-shaped

(KCT,HWC,CPH) Dept. of Civil Eng., Natl. Taiwan University, Taipei, Taiwan, ROC
(YFS), Dept. of Civil Eng., National Central University, Chonglee, Taiwan, ROC

plate has been successfully applied in the energy-absorbing restrainers for piping systems in nuclear power plants (Kelly and Skinner 1980). Recent research results have indicated that steel triangular-shaped plates cast as the added damping and stiffness device possess adequate stiffness and strength; however, the ductility and the energy dissipation capacities of the cast steel device may not be adequate to survive a severe earthquake (Su 1990). Therefore, a combined experimental and analytical investigation on the effectiveness of steel welded triangular-plate added damping and stiffness (TADAS) device was conducted at National Taiwan University (Tsai et al. 1992, Tsai and Chen 1992). Recently, advancement in detailings and fabrication of welded TADAS device has also been made and documented (Tsai et al. 1993a).

In this paper, cyclic loading test results of eleven welded TADAS devices are discussed. Test results indicate that the steel TADAS device using the proposed welding details can sustain a large number of yielding reversals without any sign of stiffness or strength degradation. The effectiveness of the proposed TADAS device on the seismic response of building structures is further illustrated by using pseudodynamic testing techniques for a two-story full-scale steel frame. From these tests, it is demonstrated that the mechanical properties of the proposed device is highly predictable. It is therefore a promising alternative for buildings intended for severe seismic service. In order to gain insight into the effects of some important parameters on the seismic response of ADAS structural systems, nonlinear response spectra for SDOF systems were analyzed. Based on these experimental and analytical studies, a design methodology and an example are developed for the design of beams, columns and braces in structures using the TADAS device as the primary energy dissipation system. The proposed design procedures, which incorporate the capacity design concepts and the optimal strength ratio of the entire ADAS frame to that of the device, can be conveniently implemented into the design of structures for improved earthquake resistance.

BASIC MECHANICAL CHARACTERISTICS OF TADAS DEVICE

As shown in Fig. 1, when a finite end displacement is imposed perpendicular to the plane of an one-edge fixed triangular plate, the bending curvature is uniformly distributed. Therefore, yielding can occur simultaneously over the full height of the plate without curvature concentration. Assuming the base of the triangular plate is fully restrained and neglecting the shear deformation, the theoretical elastic lateral stiffness of a TADAS device is:

$$K_d = \frac{N\,E\,b\,t^3}{6\,h^3} \tag{1}$$

where E is the Young's modulus, N is the number of the triangular plates, t is the plate thickness, b and h are the base width and the height of the triangular plate, respectively. The yield strength, P_y, and the plastic strength, P_p, of the device are:

$$P_y = \frac{F_y\,N\,b\,t^2}{6\,h} \tag{2}$$

$$P_p = \frac{F_y\,N\,b\,t^2}{4\,h} \tag{3}$$

and the yield displacement, Δ_y, is:

$$\Delta_y = \frac{F_y\ h^2}{E\ t} \tag{4}$$

where F_y is the tensile yield stress. If the rotational angle, γ, of the device is defined as the ratio between the lateral displacement and the height of the triangular plate, then the yield rotational angle, γ_y, is:

$$\gamma_y = \frac{F_y\ h}{E\ t} \tag{5}$$

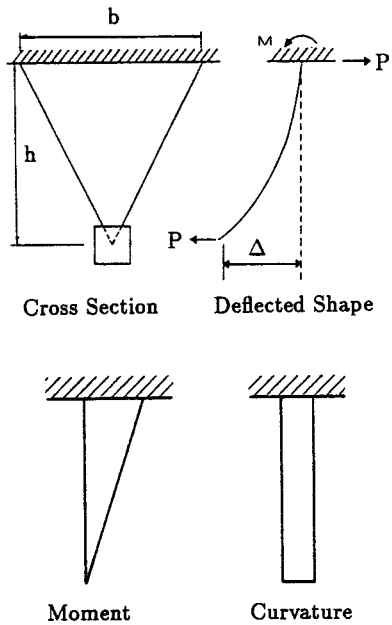

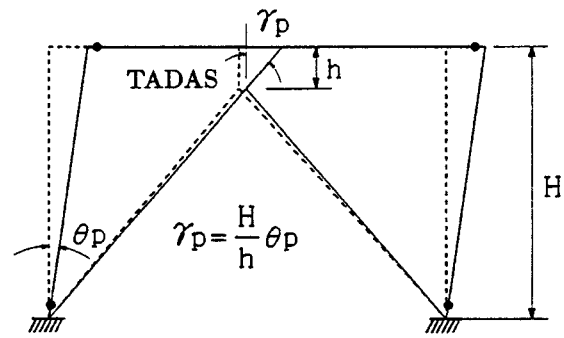

Fig. 2 Energy dissipation mechanism

Fig. 1 Basic behavior of triangular plate under load

It can be found From Eqs. 1 to 5 that the height-to-thickness ratio, h/t, of the plate is an important parameter to the mechanical properties of TADAS device. It is clear in Eq. 1 that the stiffness of the device increases rapidly as the height of the plate decreases or the thickness of the plate increases. Further more, it is possible to choose a small h/t ratio for the plate to obtain a large device stiffness while changing the height and thickness of the plate simultaneous to achieve a specific yield displacement (Tsai and Chen 1992). When properly combined with the braces in a frame, the TADAS element can be proportioned to provide not only additional frame lateral stiffness but also hysteretic damping when specific frame response is exceeded. For the purpose of discussion, an ADAS frame is defined as a frame constructed with the TADAS device. Assuming rigid plastic behavior of the members, Fig. 2 shows the energy dissipation

mechanism for an ADAS frame. From the geometry of the mechanism, the inelastic rotational demand of a TADAS device can be computed as follows:

$$\gamma_p = \frac{H}{h}\,\theta_p \tag{6}$$

where H is the story height and θ_p is the frame's plastic drift angle. Note that the rotation of the beam at the TADAS device, and the deformation of braces are neglected in Eq. 6. From Eq. 6, it is obvious that the inelastic rotational demand of the TADAS device grows as plate height decreases. When a frame drift angle of ± 0.02 radian is reached in a severe earthquake, a rotational demand in the order of ± 0.20 radian is likely to occur for a typical H/h ratio of 10.

EXPERIMENTAL INVESTIGATIONS

The proposed TADAS device consists of several triangular plates welded to a common base plate as shown in Fig. 3. In this detail, each triangular plate is inserted into the slotted base plate before fillet welds are applied to attach the triangular plate. In order to assess the mechanical properties, ductility capacity as well as the effectiveness of the proposed welded TADAS devices for building structures in regions of high seismic risk, an experimental research program was carried out (Tsai et al. 1992).

Table 1 Schedule of TADAS device specimens

TADAS Device (1)	t (mm) (2)	h (mm) (3)	b (mm) (4)	N (5)	gap (mm) (6)	Δ_y (mm) (7)	P_y (KN) (8)	P_p (KN) (9)
1A1	20	130.2	150	8	5	1.06	182.4	273.6
1A2	20	219.5	150	8	13	2.88	107.9	161.85
1A3	20	305	150	8	13	5.48	77.5	116.25
1B1	35	189	150	8	5	1.2	357	535.5
0B2	35	304	150	8	5	3.11	222.6	333.9
1B2	35	304	150	8	5	3.11	222.6	333.9
1B3	35	414.5	150	8	5	5.8	162.8	244.2
2B2	36.1	304	133.3	8	13	3.11	210	315
3B2	36	304	133.3	5	13	3.11	130.7	196.05
1C1	36	325	177.6	8	13	3.6	260.2	390.3
1C2	36	325	178.5	5	13	3.6	163.5	245.25

Cyclic Loading Tests of TADAS Device

The schedule of eleven welded TADAS device specimens of various plate height to thickness ratios is given in Table 1. All steel is of ASTM A36 material. The experimental

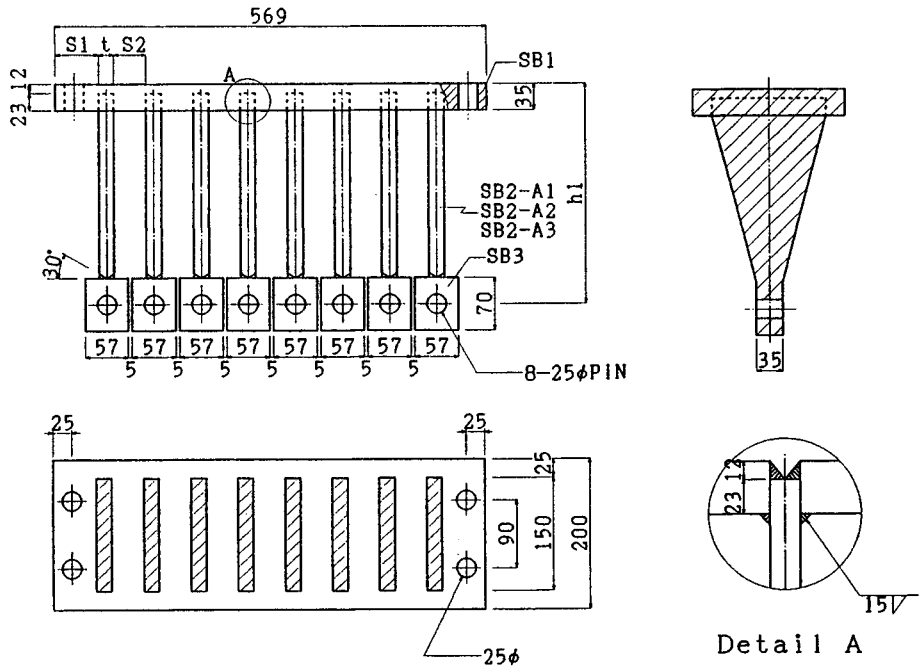

Fig. 3 Details of steel welded TADAS device (units in mm)

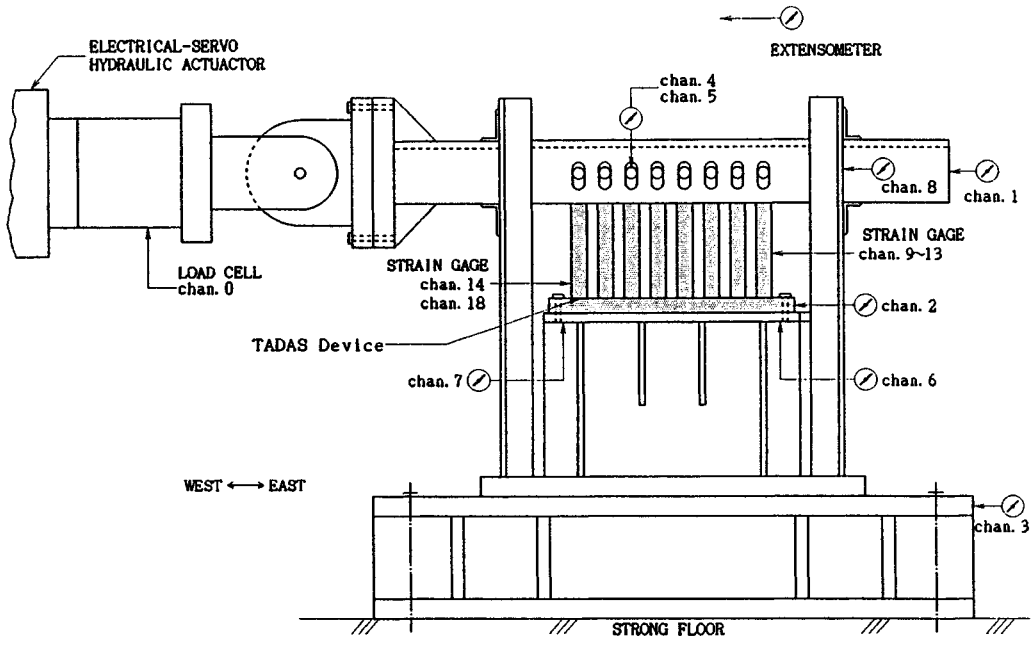

Fig. 4 Experimental set-up for cyclic test of TADAS devices

set-up for cyclic loading tests of TADAS device is illustrated in Fig. 4, where each end of the triangular plate was pin-connected to the horizontal channel through vertical slotted holes. Cyclically increasing or cyclically constant displacements were applied by connecting the horizontal channel to a servo-controlled hydraulic actuator. The cyclic force versus deformation relationships of typical TADAS device specimens are shown in Fig. 5. It can be seen from the figure that a properly welded steel TADAS device can sustain a large number of yielding reversals without any sign of stiffness or strength degradation. Except Specimen 0B2, where a less effective welding detail was used in attaching the triangular plate (Tsai 1992), failed before a rotational angle of 0.16 radian was attained, the rotational capacity of a typical TADAS device tested is generally larger than ± 0.25 radian under cyclically increased loads. It is also exhibited in Fig. 5 that the elastic stiffness of the proposed TADAS device is very predictable by considering flexural deformation only. Under cyclically increased loads, it is evident that the effects of strain hardening are very pronounced when large deformations are developed in the device. The strain hardening factor, computed by dividing the actual strength by the plastic strength, P_p, is generally on the order of 1.5 when a rotational angle of ± 0.20 radian is reached.

Pseudodynamic Tests of A Two-Story Steel ADAS Frame

The effectiveness of the TADAS device for buildings in high seismic risk were further investigated using pseudodynamic testing procedures for a two-story steel frame. Fig. 6 shows the dimensions and member sizes of the test frame. All steel is of ASTM A36 material. Fig. 7 shows the general view of the test frame. The TADAS devices used in the first and second levels are identical to Specimens 1C1 and 1C2, respectively, given in Table 1. A mass of 0.019 $ton - sec^2/mm$ was assumed for each floor. The central-difference integration scheme using dual displacement control technique (Shing and Mahin 1984) was implemented in this two degree-of-freedom pseudodynamic test program. During the course of the study, seismic responses of the frame without the TADAS devices being activated were also investigated by removing the connecting pins between the device and the braces. The first and second mode periods of the frame without the TADAS devices activated are 0.881 and 0.237 seconds, respectively. The first and second mode periods of the frame with the TADAS devices are 0.573 and 0.201 seconds, respectively.

As shown in Fig. 8, the elastic frame responses under the north-south component of the 1940 El Centro Earthquake (EC) scaled to a peak ground acceleration (PGA) of 50 cm/sec^2 were greatly reduced when the TADAS devices were activated. In order to study the elastic and inelastic responses of the ADAS frame, several earthquake ground acceleration records with different intensities were used in this study. Here, only some important observations from the tests of the ADAS frame under the 1978 Miyagi-Ken-Oki (MO) Earthquake, scaled to a PGA of 80 cm/sec^2 (Event MO80) and El Cnetro Earthquake scaled to a PGA of 312 cm/sec^2 (Event EC312) are presented. As revealed in Fig. 9 for Event MO80, the maximum story drift angle is smaller than 0.003 radian. As revealed in Fig. 10 for Event EC312, the maximum upper story drift angle is 0.016

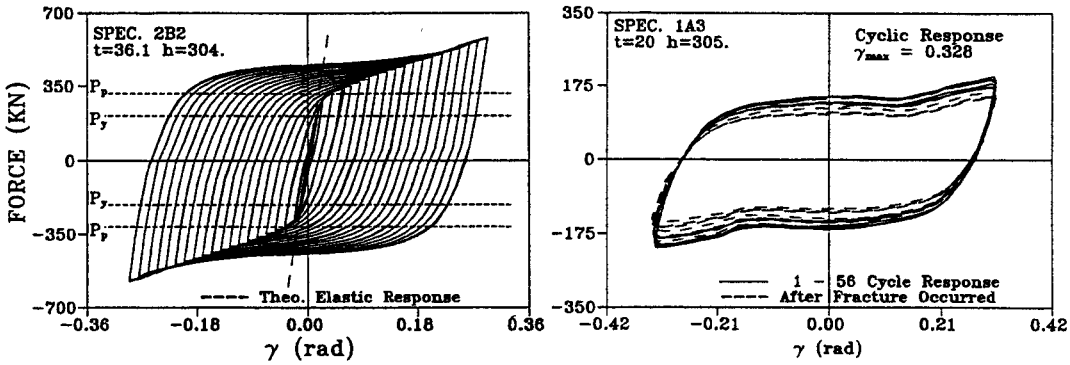

Fig. 5 Force versus deformation relationships of typical welded TADAS devices

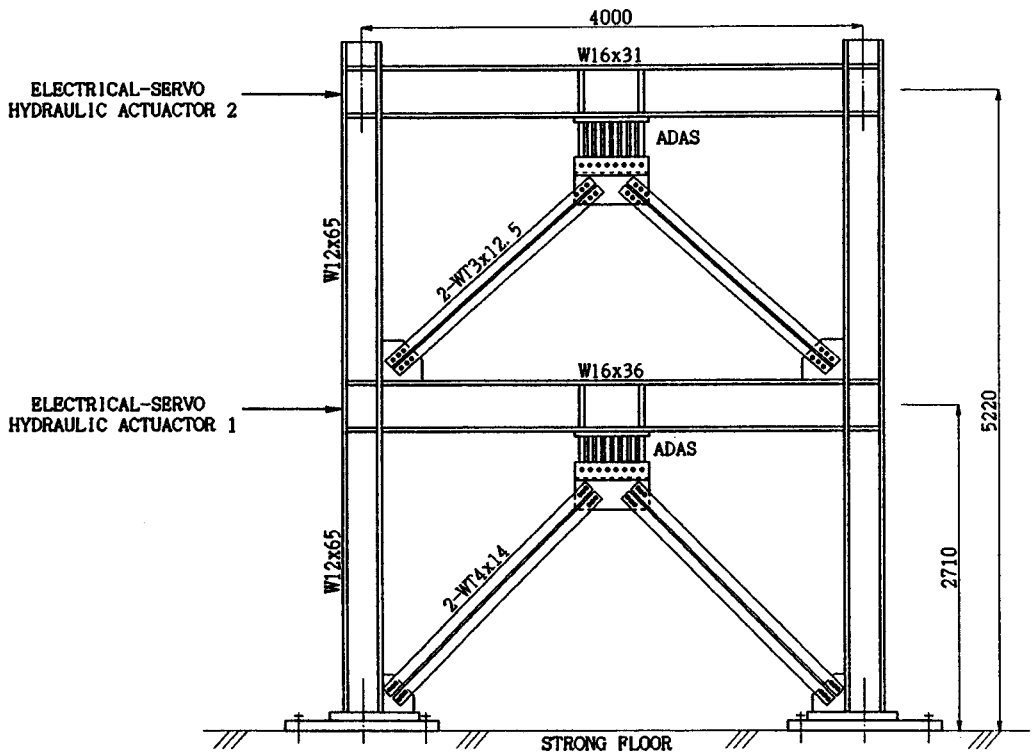

Fig. 6 Experimental set-up of pseudodynamic testing of a 2-story TADAS frame

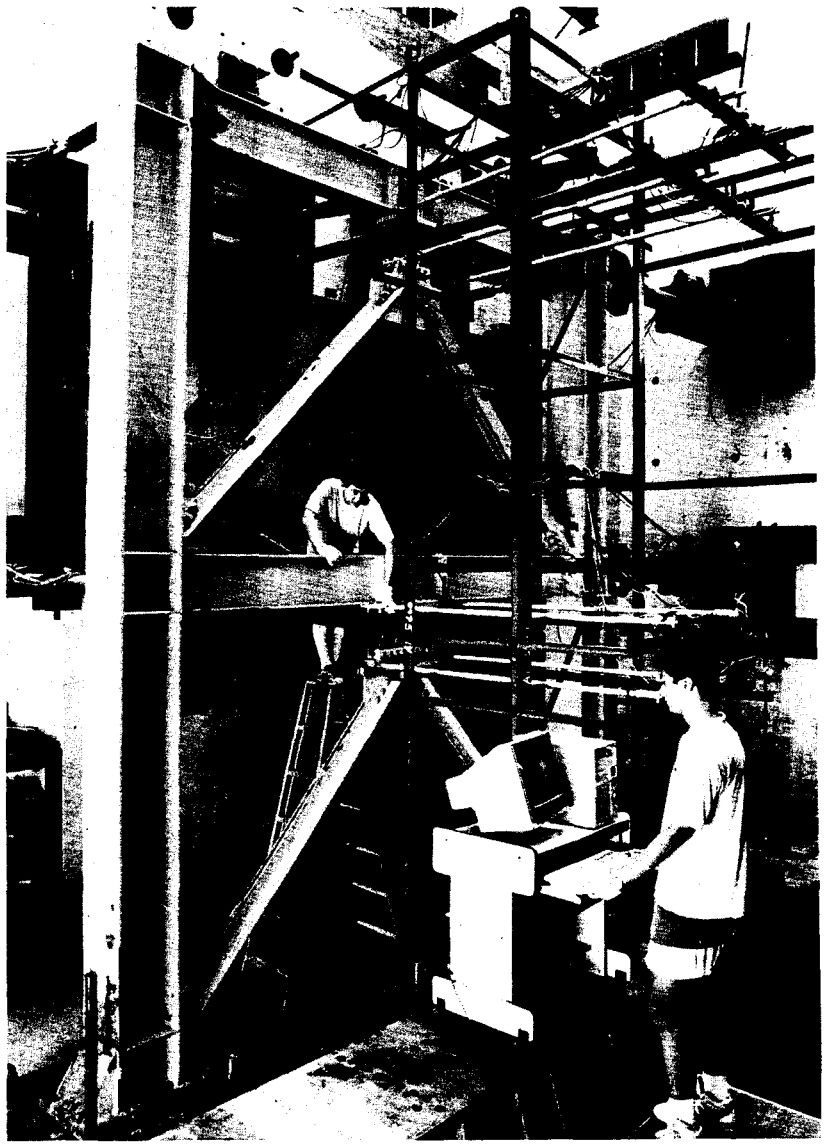

Fig. 7 A view of the test frame

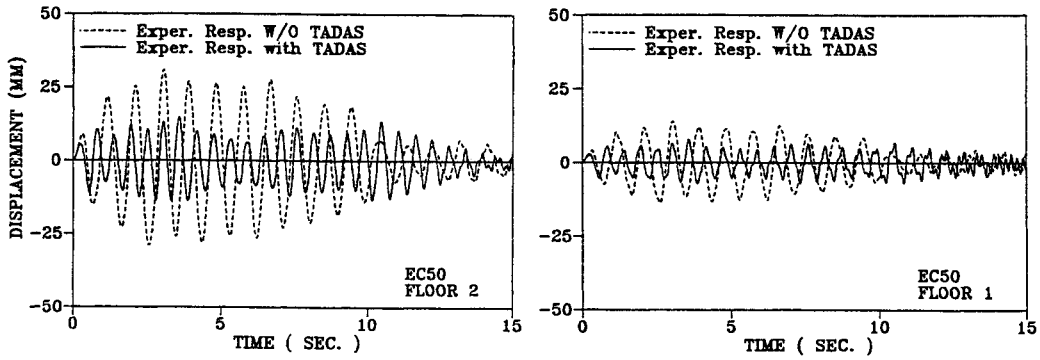

Fig.8 Pseudodynamic responses of the frame with and without the device

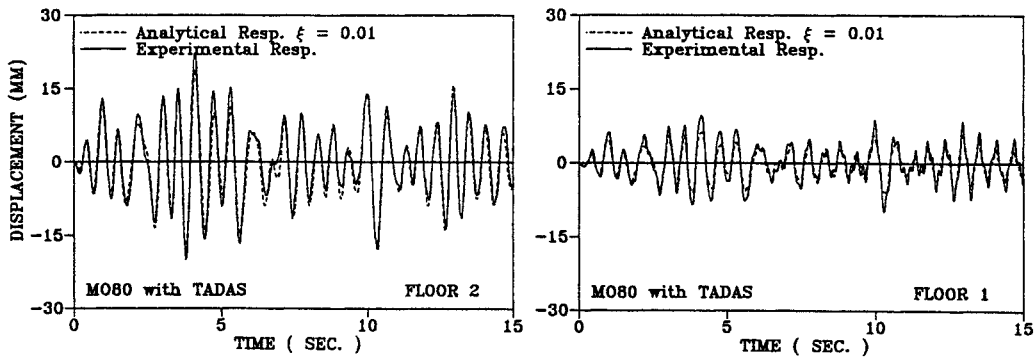

Fig. 9 Pseudodynamic responses of the ADAS frame under Event MO80

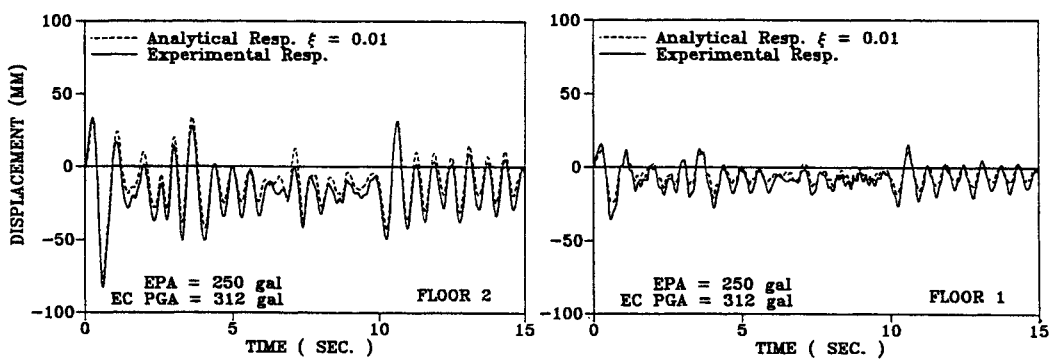

Fig. 10 Pseudodynamic responses of the ADAS frame under Event EC312

radian while the maximum TADAS rotational demand is only 0.14 radian (not shown), which is much less than the rotational capacity of all the TADAS devices tested.

In Figs. 9 and 10, the experimental results were also compared with the analytically predicted responses. A viscous damping ratio of 0.01 was assumed for all pseudodynamic tests and the corresponding analyses of the frame. In these analyses, the TADAS device was modeled by an equivalent prismatic beam element with the elastic stiffness and the plastic strength equivalent to those given in Eqs. 1 and 3. The bilinear moment-rotation relationships for the equivalent beam element and the DRAIN-2D (Kannan and Powell 1973) computer program were employed. Since the frame had gone through several tests where inelastic deformation and strain hardening of TADAS devices had occurred, the analytical predicted responses do not exactly agree with the experimental results shown in Fig. 10. However, considering the much better agreements than that shown in Fig. 10 in other inelastic tests not discussed in this paper and that the simple beam model adopted for the TADAS device, the overall agreements between these analytical and experimental responses are very satisfactory.

Design Implications

Note that one of the most attractive features in the proposed TADAS element is that the effects of gravity load in the frame can be completely separated from the seismic energy absorbing device by using the slotted holes in the connection details shown in Fig. 11. Furthermore, under large deformations of the device, the vertical displacements at the end of the triangular plate can be easily accommodated. Therefore, the plasticity within the triangular plate is very straight forward and, as evident in the previous analyses, the inelastic response of the proposed TADAS device is highly predictable.

It is important to note that the lateral supports for the TADAS device were indirectly provided by restraining the beam as shown in Fig. 11. It was judged that the triangular plate is relatively stiff in the direction parallel to the plane of the plate and that the roller end is free to rotate. Therefore, lateral support near the roller end of the device was eliminated. In order to maintain the stability of the braces in the out of plane, shim plates were placed between the pin block and the slotted side plates as shown in Fig. 12. During all pseudodynamic tests of the ADAS frame, no instability of the member was observed. Since the direct lateral support at the roller end of the TADAS device can be eliminated by using the proposed connection detail, therefore, this is a very attractive architectural feature where large ceiling height in the building is to be maintained.

RESPONSE ANALYSIS OF SDOF ADAS FRAMES

The influence of various ADAS element parameters on seismic response of building structures has been extensively analyzed (Xia and Hanson 1992). In order to gain further insight into the effects of some important TADAS parameters on the seismic response

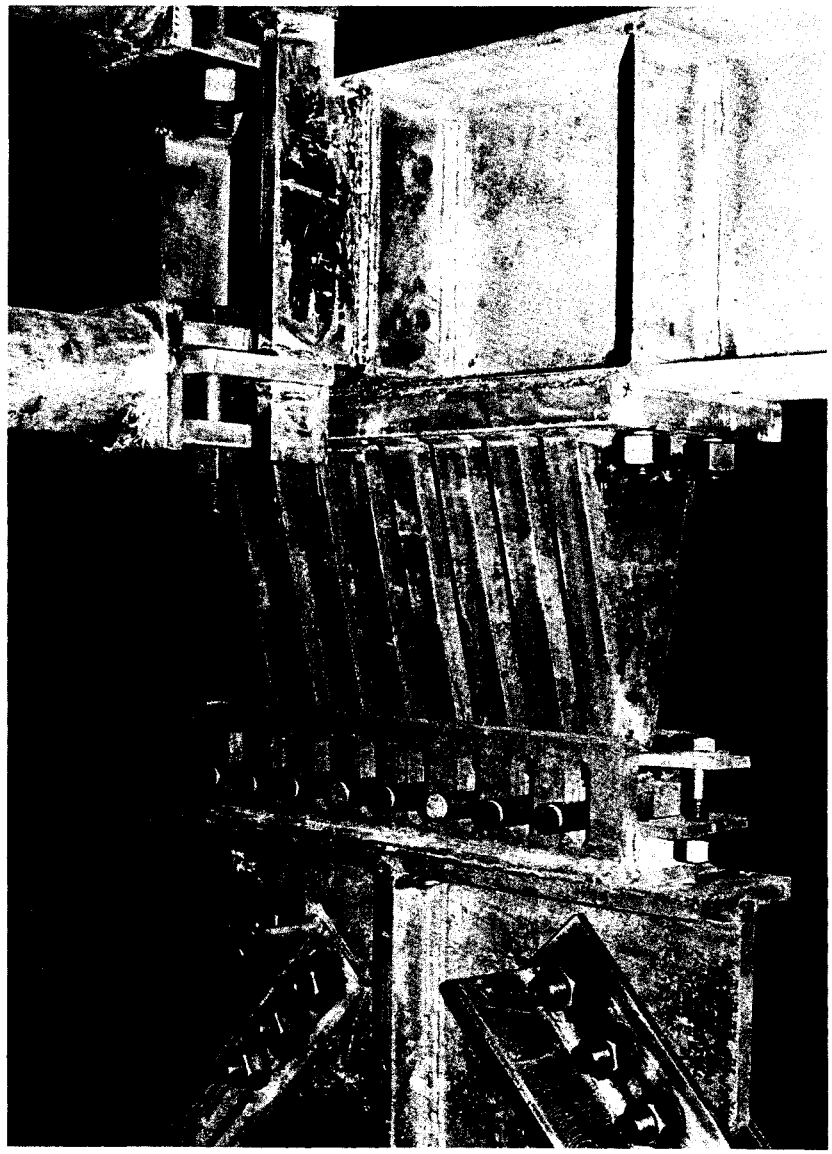

Fig. 11 TADAS device-to-brace connection details

of building frames, nonlinear response spectra of SDOF system were studied (Tsai and Chen 1992, Tsai et al. 1993b). For the purpose of discussion, a TADAS element is defined as a TADAS device and two braces that support the device. The horizontal stiffness of the TADAS element, K_a, is a function of the lateral stiffness of the braces, K_b, and the device stiffness, K_d. If the ratio of the horizontal TADAS element stiffness, K_a, to the structural story stiffness without the TADAS device and braces in place, K_f, is defined as SR (Xia and Hanson 1992), then:

$$SR = \frac{K_a}{K_f} \tag{7}$$

and

$$K_a = \frac{K_b K_d}{K_b + K_d} \tag{8}$$

Since generally the device will yield before the frame undergoes inelastic deformations, it has been found that the force-deformation relationships of a steel frame with the TADAS device can be adequately characterized by a tri-linear model as shown in Fig. 13 (Tsai and Chen 1992). In the figure, the elastic stiffness, K_S, of the ADAS frame is:

$$K_S = K_a + K_f$$

In addition, $\Delta_y 1$ and $\Delta_y 2$ represent the yield displacements of the TADAS element (with braces) and the frame without the TADAS element (device and braces) in place, respectively; $R_y 1$ and $R_y 2$ represent the total restoring forces developed in the system when $\Delta_y 1$ and $\Delta_y 2$ are reached, respectively. Let SHR_A be defined as the ratio of the TADAS element (with braces) stiffness after yield to the initial element stiffness. That is, the post yield stiffness of the TADAS element (with braces) is $Ka \times SHR_A$. Also let:

$$U = \frac{R_y 2}{R_y 1} \tag{9}$$

Since

$$K_a = SR \times K_f \tag{10}$$

$$R_y 1 = (K_a + K_f)\Delta_y 1 \tag{11}$$

$$R_y 2 = K_f \Delta_y 2 + K_a \Delta_y 1 + SHR_A K_a (\Delta_y 2 - \Delta_y 1) \tag{12}$$

Therefore, from Eqs. 9, 11 and 12,

$$U = \frac{K_f \Delta_y 2 + K_a \Delta_y 1 + SHR_A K_a (\Delta_y 2 - \Delta_y 1)}{(K_a + K_f)\Delta_y 1} \tag{13}$$

Then, from Eq. 13,

$$\frac{\Delta_y 2}{\Delta_y 1} = \frac{UK_a + UK_f + K_a SHR_A - K_a}{K_f + K_a SHR_A} \tag{14}$$

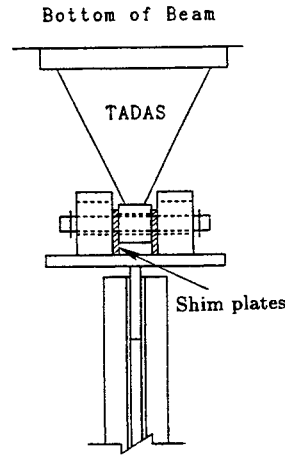

Fig. 12 Shim plates in the device-to-brace connection

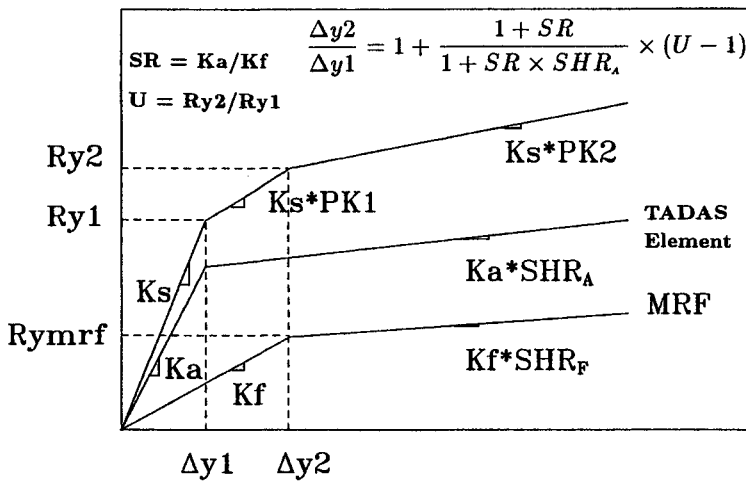

Fig. 13 Tri-linear force versus deformation relationships of the TADAS frame system

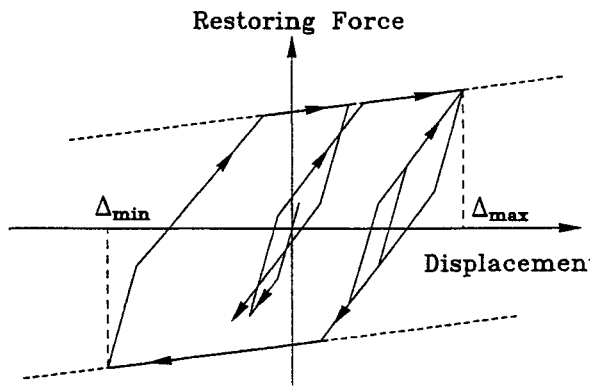

Fig. 14 Tri-linear hysteresis rules for the TADAS frame system

Substitute Eq. 10 into Eq. 14, then the relationship between $\Delta_y 1$, $\Delta_y 2$, SR, U and SHR_A is:

$$\frac{\Delta_y 2}{\Delta_y 1} = 1 + \frac{1 + SR}{1 + SR \times SHR_A} \times (U - 1) \tag{15}$$

Based on Eq. 15 and using the hysteresis rules as shown in Fig. 14 implemented into a nonlinear response spectrum analysis program (Mahin and Lin 1983), the acceleration, displacement, input energy and the ductility response spectra were extensively studied for SDOF ADAS frame systems under four historical earthquake excitations scaled to an effective peak ground acceleration of 400 cm/sec^2 (Tsai and Chen 1992, Tsai et al. 1993b). It is found from these analyses that the most important parameters affecting the seismic responses of the ADAS frame include the stiffness ratio, SR, the strength ratio, U, and the frame lateral displacement when device yields, $\Delta_y 1$. It is important to note that the inclusion of the TADAS element will reduce, as a function of the SR value, the vibration period of the corresponding frame without the TADAS element in place. Therefore, it requires systematic relating the responses of different ADAS frames (of various SR values) to the corresponding bare frame (with one specific vibration period) in order to assess the effects of the stiffness ratio SR on the structure. As the TADAS element may significantly change the frame vibration period, the effects of the SR ratio on the seismic response of the ADAS frames are also sensitive to the frequency contents of the earthquake excitations (Tsai and Chen 1992). Thus, it is difficult to draw absolute conclusions from the results of these spectral analyses. However, the general trend found from the spectral responses of the SDOF ADAS frame can be summarized as follows (Tsai et al. 1993b):

1. the responses of the system are not sensitive to the strain hardening ratios,

2. the larger the SR value the smaller the displacement response will occur and the larger the acceleration response may result,

3. the larger the SR value the smaller the total energy input will result for systems of short vibration period,

4. the smaller the SR value the smaller the ductility demand on the device will result for systems of medium to long vibration period.

Based on these studies, it is found that a strength ratio U of about 2 is optimal, SR values less than 4 and 2 are appropriate for systems of short and medium to long vibration periods, respectively.

DESIGN OF EARTHQUAKE-RESISTANT ADAS FRAMES

One of the most attractive features in applying the proposed TADAS device is that the effects of gravity load can be completely separated from the primary lateral force resisting elements by using the slotted holes in the brace-to-device connections as shown in Fig. 11. Furthermore, it should be recognized that the most important concept

of seismic resistant ADAS frame design is that the yielding and damage to the frame can be restricted primarily to the TADAS devices. Therefore, following capacity design principles, the braces, columns and the beams supporting the device must be designed for the maximum forces generated by the device, accounting for the effects of strain hardening.

Since the ductility capacity of a properly fabricated TADAS device is more than adequate for practical applications in a seismic-resistant frame, a large R_w factor similar to that used for the seismic eccentrically braced frame may be adopted for the computation of design seismic force (ICBO 1991). Recent research results have indicated that ductile structural system designed based on the model seismic force provisions may go well into inelastic deformations under a "moderate" earthquake (Uang 1991). Therefore, a practical design procedure, incorporating the research results described above and the seismic-resistant design concept adopted in the Japanese Building Standard Law (International Association for Earthquake Engineering 1988), is devised for the construction of seismic-resistant ADAS frame systems as follows:

1. Establish the site-dependent service level design earthquake, an event corresponding to an effective peak ground acceleration of 80 cm/sec^2 for buildings in regions of high seismic risk is generally adopted.

2. Select a suitable SR value based on the fundamental period estimated for the frame.

3. Proportion the frame without the TADAS element in place. A moment resisting frame (MRF) capable of resisting at least 25% of the prescribed seismic force is recommended. Compute the lateral stiffness, K_f, of each floor. Compute the yield displacement of the bare frame, $\Delta_y 2$.

4. Compute the TADAS element stiffness, K_a, from Eq. 10 and the yield displacement of the device, $\Delta_y 1$, from Eq. 15 for the selected SR, SHR_A and an U value of 2. Design the TADAS device for each floor based on the device yield displacement $\Delta_y 1$ and the stiffness K_d from Eq. 8 for given K_a and K_b. Incorporate the TADAS elements into the frame obtained from Step 3.

5. Perform lateral force analyses for the frame with the TADAS element in place using the design earthquake given in Step 1. When necessary, repeat Steps 3 and 4 to meet member strength and frame drift requirements for serviceability limit state.

6. Perform capacity design checks for the braces, columns and beams assuming the ultimate force generated in the device is $1.5P_p$, where P_p is define in Eq. 3.

It is important to note that if the overstrength factor is defined as the ratio of the actual strength to the strength at first significant yield of the system (Uang 1991), then an overstrength factor of the system greater than 2 is ensured when a strength ratio

$U = 2$ is selected in the proposed design procedure.

DESIGN EXAMPLE

The example structure is a three bay, 20-story plane frame, with TADAS elements in the central bay as shown in Fig. 15. The design dead weight is 36 KN/m and the design live load is 12 KN/m, uniformly distributed over the beam span in each floor. To illustrated the effectiveness of the proposed design procedure, the 1978 Miyagi-Ken-Oki earthquake scaled to PGA of 111 cm/sec^2 (Event MO111 and EPA=80 cm/sec^2) and 555 cm/sec^2 (Event MO555 and EPA=400 cm/sec^2) are adopted as the design serviceability and collapsibility limit state events, respectively. The detailed design procedures of the example frame are as follows:

1. Construct the elastic acceleration response spectrum for Event MO111 using 2% of critical damping.

2. Since a 20-story frame should have a medium fundamental period, a stiffness ratio of $SR = 2$ and a strength ratio of $U = 2$ are chosen.

3. Perform preliminary member design for the frame without the TADAS element in place. The ETABS computer program (Habibullah 1991), which incorporates the complete quadratic modal combination (CQC) algorithm, is used to perform the dynamic analyses. Compute the lateral stiffness, K_f, of each floor for the resulting frame. The yield displacement of the bare frame, $\Delta_y 2$, can be obtained from a nonlinear static response analysis. In lieu of such analysis, an approximate approach is adopted in this study. This is accomplished by assuming rigid-plastic behavior for the MRF and using the lateral force distribution pattern obtained from the associated elastic dynamic analysis. Assume the ratio between the story yield force and the CQC story force (F_i) obtained from the elastic analysis is α. As shown in Fig. 16, let H_i and F_i be the floor height and the CQC story force of the ith floor, respectively. Then, using the principle of virtual work, the yield forces of the entire frame, $\alpha\Sigma F_i$, are estimated as follows:

$$\alpha\Sigma(F_i \times H_i \times \theta_p) = \Sigma M_{pj} \times \theta_p \tag{16}$$

The left hand side of Eq. 16 considers the external work produced by all story forces. The right hand side of Eq. 16 takes sum over the plastic hinge, of plastic moment capacity M_{pj}, at all beam ends and the base of all columns. The yield displacement, $\Delta_y 2$, of each story is obtained by applying all frame yield forces, αF_i, at the corresponding floors and performing an elastic static analysis for the 20-story frame.

4. Compute the TADAS element stiffness, K_a, from Eq. 7 using $SR = 2$ and K_f obtained from Step 3 for each floor. Based on $SR = 2$, $U = 2$, $SHR_A = 0.05$, K_f and $\Delta_y 2$ obtained from step 3, compute the yield displacement, $\Delta_y 1$, of the device from Eq. 15 for each floor.

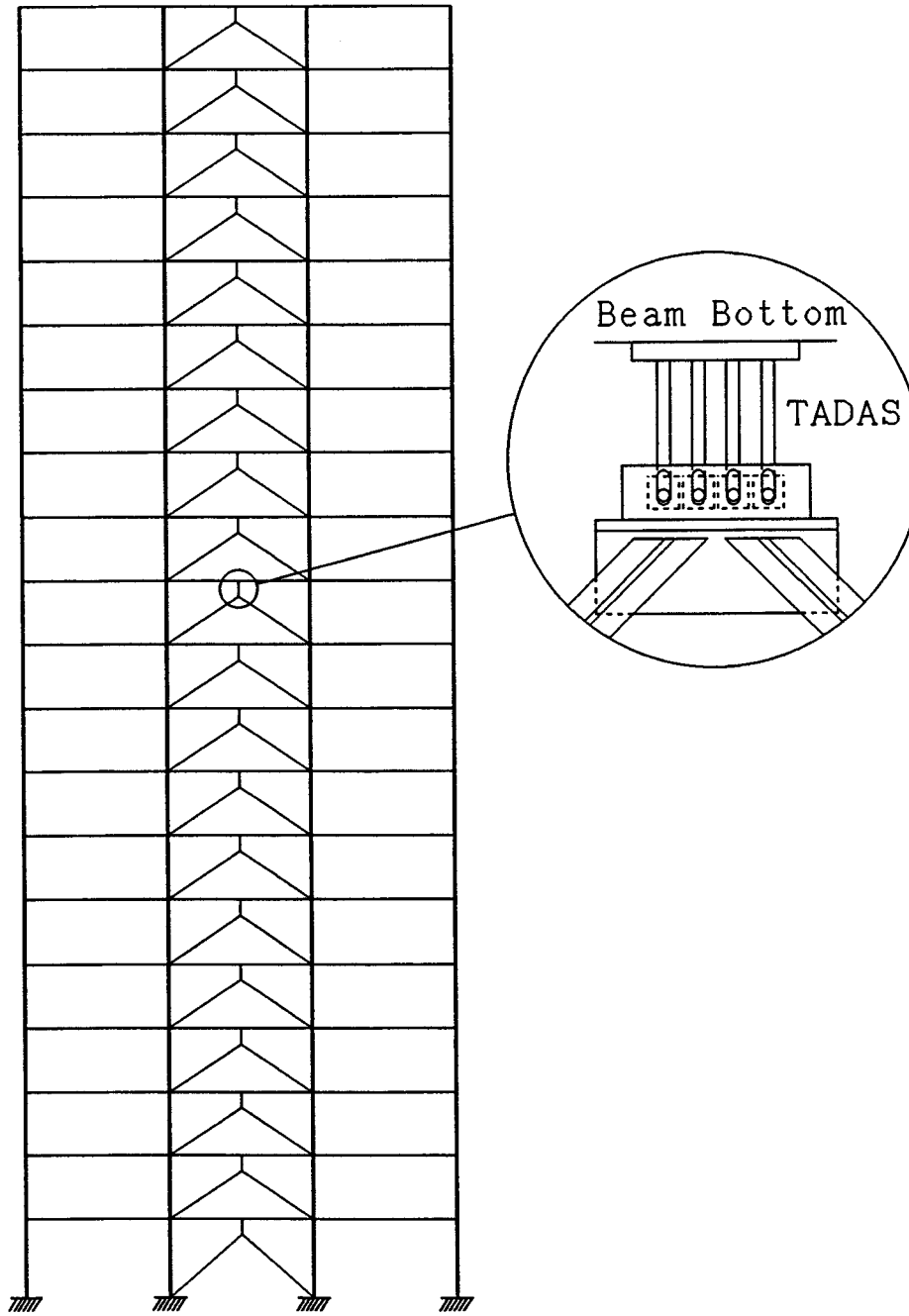

Fig. 15 Elevation of a 3-bay 20-story ADAS frame

Table 2 Schedule of beams, columns and braces

FL	COLUMN LINE		BEAM BAY		BRACE
	C1&C4	C2&C3	B1&B3	B2	
RF	W12X106	W14X176	W24X94	W24X94	2-WT7X26.5
19F	DO	DO	DO	W24X94	2-WT7X37
18F	DO	DO	W24X94	W24X117	2-WT7X45
17F	W12X106	W14X176	W24X104	DO	2-WT7X45
16F	W14X109	W14X193	DO	DO	2-WT7X49.5
15F	DO	DO	W24X104	W24X117	2-WT7X49.5
14F	DO	DO	W27X114	W27X146	2-WT7X54.5
13F	W14X109	W14X193	DO	DO	2-WT7X54.5
12F	W14X120	W14X211	DO	DO	2-WT7X60
11F	W14X120	DO	DO	DO	DO
10F	W14X132	DO	DO	DO	DO
9F	W14X132	W14X211	W27X114	W27X146	2-WT7X60
8F	W14X145	W14X257	W30X124	W30X173	2-WT6X76
7F	W14X145	DO	DO	DO	DO
6F	W14X159	DO	DO	DO	DO
5F	W14X159	W14X257	DO	W30X173	2-WT6X76
4F	W14X176	W14X283	DO	W30X211	2-WT6X85
3F	W14X176	W14X283	DO	DO	2-WT6X85
2F	W14X211	W14X342	DO	DO	2-WT6X95
1F	W14X211	W14X342	W30X124	W30X211	2-WT7X66

Table 3 Schedule of TADAS devices

FL	K_f (kN/m)	K_a (kN/m)	$\triangle_y$ (mm)	t (mm)	h (mm)	b (mm)	N
RF	76220	152439	3.1	50	351	350	7
19F	78370	156740	4.4	50	419	350	10
18F	78989	157978	5.3	50	476	350	15
17F	81433	162866	5.6	50	476	350	15
16F	88889	177778	5.6	50	476	350	18
15F	91324	182648	5.6	50	476	350	18
14F	98328	196657	5.6	50	476	350	18
13F	98814	197629	5.6	50	476	350	18
12F	105708	211416	5.6	50	476	350	20
11F	106045	212089	5.6	50	476	350	20
10F	108460	216920	5.6	50	476	350	20
9F	111857	223714	5.6	50	476	350	20
8F	136240	272480	5.6	50	476	350	26
7F	137174	274348	5.6	50	476	350	26
6F	140253	280505	5.6	50	476	350	26
5F	141443	282885	5.6	50	476	350	26
4F	152439	304878	5.6	50	476	350	28
3F	155280	310559	5.6	50	476	350	29
2F	176367	352734	5.6	50	476	350	33
1F	121507	243013	5.6	50	476	350	23

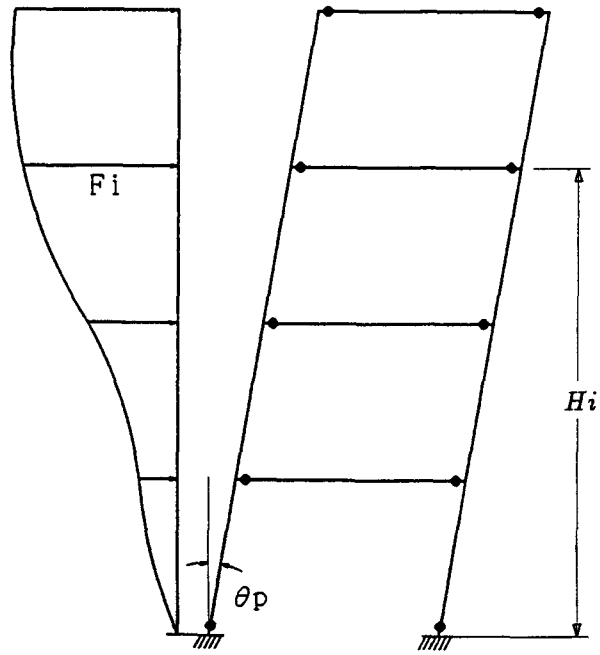

Fig. 16 Determination of ultimate lateral strength using frame sway mechanism

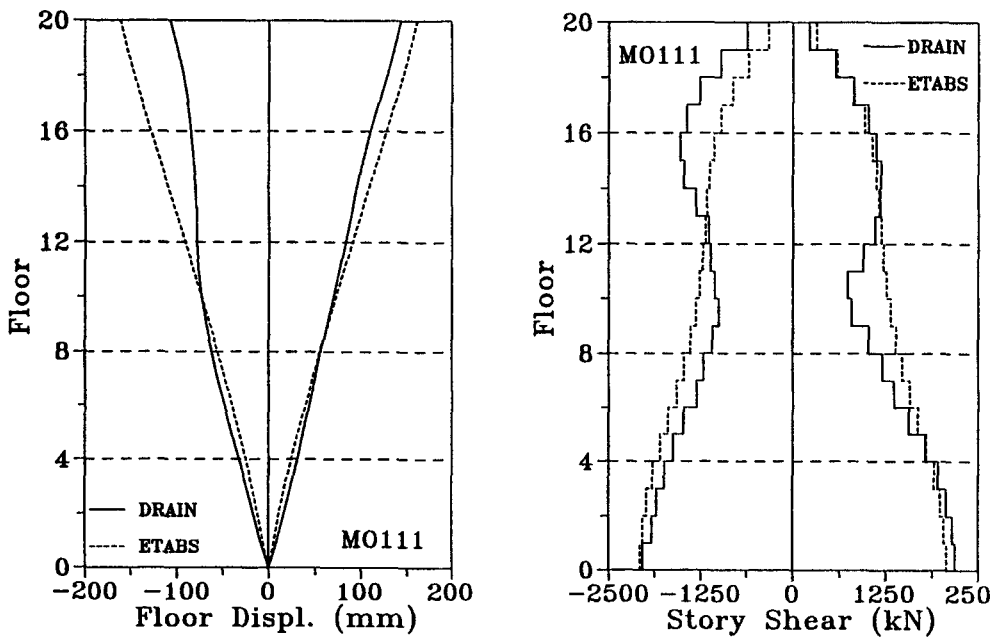

Fig. 17 Comparison of story displacements and story shears

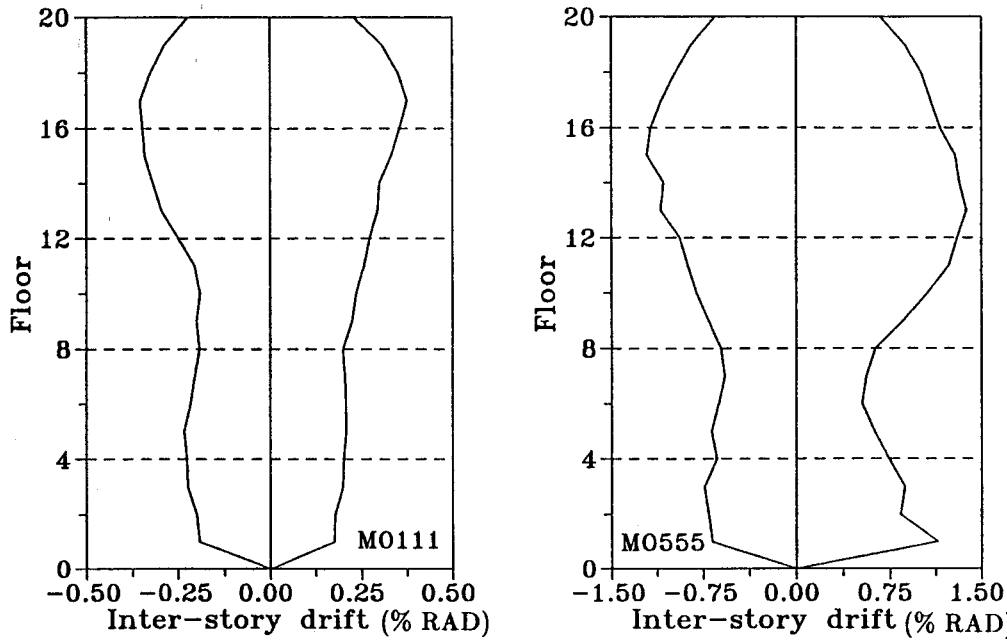

Fig. 18 Story drifts under Events MO111 and MO555

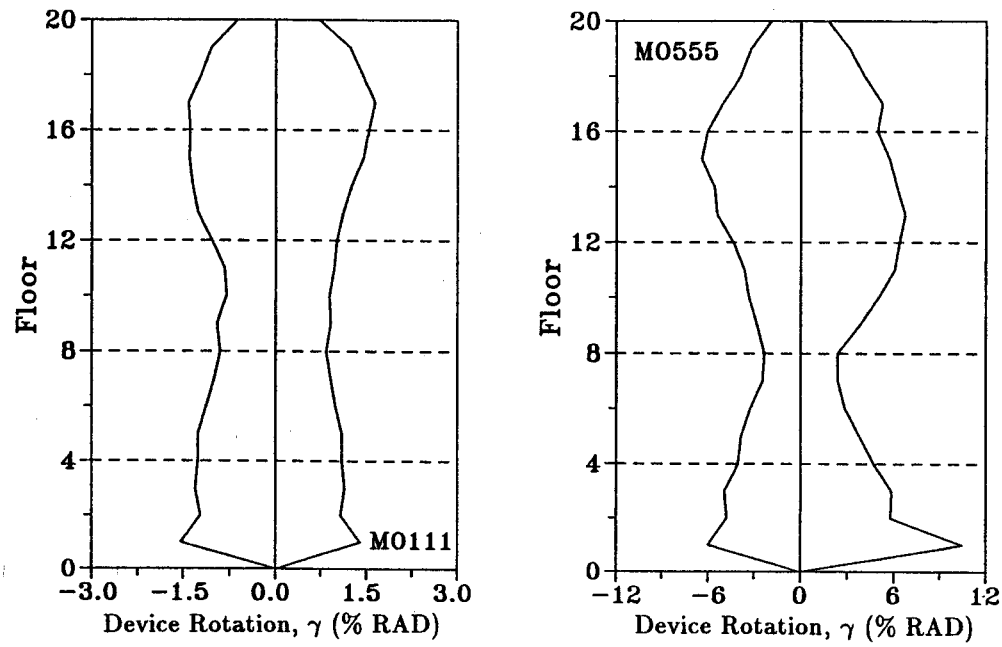

Fig. 19 TADAS Rotations under Events MO111 and MO555

5. Construct a 20-story concentrically braced frame (CBF) in which the lateral stiffness of each pair of concentric braces is equivalent to K_a. Using the design response spectrum constructed in Step 1, perform dynamic response analyses for the equivalent CBF. Check member strength and story drifts in order to meet serviceability limit state requirements. In this example, member stresses are limited within 1.5 times the allowable stress (AISC 1989) under the combined gravity loads and the prescribed seismic forces; a story drift limit of 0.005 radian for serviceability is adopted. Note that without the TADAS element, the 3-Bay 20-story MRF is able to resist a minimum of 33% of the total forces induced under the Event MO111 since the stiffness ratio SR of 2 was selected.

6. Assume the TADAS device remains essentially elastic before plastic strength, P_p, is reached (Fig. 5). Thus, let $\Delta_y 1 = 1.5\Delta_y$, where Δ_y is defined in Eq. 4, proportion the TADAS device and the braces using Eqs. 1 and 8. Perform capacity design check for the braces, columns and the beams assuming the ultimate force generated in each device is $1.5P_p$.

The final selections of the member and the TADAS device are shown in Tables 2 and 3, respectively. All steel is of ASTM A36 grade. The use of an equivalent CBF in Step 5 facilitates a simple analytical model without introducing an additional node at the actual device-to-brace joint but retain accurate force distribution among the braces and columns. In order to illustrate the effectiveness of the equivalent CBF used in Step 5, the dynamic responses of the CBF obtained by using the ETABS program and the CQC algorithm in Step 5, are compared with the results obtained from the time history response analyses for the DRAIN-2D finite element model. As shown in Fig. 17 for Event MO111, the response of the equivalent CBF well agree with that obtained from the time history analysis performed for the finite element ADAS frame model.

Under the serviceability limit state earthquake, Event MO111, and the collapsibility limit state earthquake, Event MO555, the maximum interstory drift responses of each story are shown in Fig. 18. It can be found in the figure that the story drift ratios are within 0.005, and satisfy the serviceability requirement under Event MO111, and are within 0.015 radian under the collapsibility limit state earthquake. Under these two events, the rotational demands imposed on the TADAS device are given in Fig. 19. It can be found in the figure that under Event MO555, the maximum rotational demand imposed on the TADAS is only about 0.11 radian, well below the rotational capacity of a typical TADAS device tested previously.

Since it only requires conventional elastic frame response analysis computer program in the design steps described above, the proposed design procedures can be conveniently applied in a regular structural design office.

CONCLUSIONS

Based on these studies, several conclusions can be drawn as follows:

- Elastic stiffness and ultimate strength of the proposed steel TADAS device can be accurately predicted.

- Rotational capacity of a properly welded TADAS device is larger than ± 0.25 radian.

- Seismic responses of building frames equipped with the proposed TADAS devices can be well controlled and accurately predicted by traditional nonlinear frame response analysis computer program. The hysteretic behavior of the TADAS device can be adequately characterized by an equivalent prismatic beam member using the elastic strain-hardened bilinear moment-rotation relationships.

- Since a nonlinear analysis can be avoided as illustrated in the design example, and that specific serviceability and overstrength requirements can be adequately satisfied, it appears that the proposed design procedures can be conveniently employed for the preliminary design of TADAS element or any other similar energy absorbing devices for improved earthquake-resistant construction. However, a nonlinear analysis would be useful for final verification of device ductilities, member forces and interstory drifts.

ACKNOWLEDGEMENTS

The authors gratefully acknowledge the supports of the National Science Council of the Republic of China (Grant No. NSC 82-0414-P-002-032-B) and the Sinotech Foundation for Research and Development of Engineering Science and Technology.

REFERENCES

AISC, (1989), "Manual of Steel Construction, Allowable Stress Design," American Institute of Steel Construction, Chicago, IL.

Bergman D.M. and Goel, S.C., (1987), "Evaluation of Cyclic Testing of Steel-Plate Device for Added Damping and Stiffness," Report UMCE 87-10, Department of Civil Engineering, University of Michigan. Ann Arbor, Michigan.

Habibullah, A., (1991), "ETABS, Three-Dimensional Analysis of Building Systems," Computer and Structures, Inc.

ICBO, (1991), International Conference of Building Officials, "Uniform Building Codes," Whittier, CA.

Kannan, A.E. and Powell, G.H., (1973), "DRAIN-2D, A General Purpose Computer Program for Dynamic Analysis of Inelastic Plane Structures," Report No. UCB/EERC-73/22, Earthquake Engineering Research Center, University of California, Berkeley.

Kelly, J.M. and Skinner, M.S., (1980), "The Design of Steel Energy-Absorbing Restrainers and their Incorporation into Nuclear Power Plants for Enhanced Safety (Vol 2): Development and Testing of Restraints for Nuclear Piping Systems," Report No.

UCB/EERC-80/21, Earthquake Engineering Research Center, University of California, Berkeley.

Mahin, S. and Lin, J., (1983), "Construction of Inelastic Response Spectra for Single-Degree-of-Freedom Systems", Report No. UCB/EERC-83/17, Earthquake Engineering Research Center, University of California, Berkeley.

Shing, P.B. and Mahin, (1984), "Pseudodynamic Test Method for Seismic Performance Evaluation: Theory and Implementation," UCB/EERC-84/01, Earthquake Engineering Research Center, University of California, Berkeley.

Su, Y.F. and Hanson, R.D., (1990), "Seismic Response of Building Structures with Mechanical Damping Devices," Report UMCE 90-2, Department of Civil Engineering, University of Michigan. Ann Arbor, Michigan.

Su, Y.F., (1990), "Aseismic Design of Building Structures with ADAS Devices," A Report to the Sinotech Foundation for Research and Development of Engineering Science and Technology, Su and Structural Engineers Corporation, Taiwan.

Tsai, K.C., Hong, C.P. and Su, Y.F., (1992), "Experimental Study of Steel Triangular Plate Energy Absorbing Device for Seismic-Resistant Structures," Report NO CEER/R81-08, Center for Earthquake Engineer Research, National Taiwan University, Taipei, Taiwan. (in Chinese)

Tsai, K.C. and Chen, H.W., (1992), "Seismic Response of Building Structures using Steel Triangular Plate Energy Dissipators," Report NO CEER/R81-09, Center for Earthquake Engineer Research, National Taiwan University, Taipei, Taiwan. (in Chinese)

Tsai, K.C., (1992), "Steel Triangular Plate Energy Absorber for Earthquake-Resistant Buildings," *Proceedings, the First World Conference on Constructional Steel Design*, Acapulco, Mexico.

Tsai, K.C., Li, J.W., Hong, C.P., Chen, H.W. and Su, Y.F., (1993a), "Welded Steel Triangular Plate Device for Seismic Energy Dissipation", *Proceedings, ATC-17-1 Seminar on Seismic Isolation, Passive Energy Dissipation, and Active Control*, San Francisco, CA.

Tsai, K.C., Chen H.W., Hong, C.P. and Wang, T.F., (1993b), "Steel Plate Energy Absorbers for Improved Earthquake Resistance", *Proceedings, ASCE Structures Congress*, Irvine, CA.

Uang, C.M., (1991), "Establishing R_W and C_d Factors for Building Seismic Provisions," Journal of Structural Engineering, ASCE, Vol 117, No. 1.

Whittaker, A., Bertero, V.V. and Alonso, J., (1989), "Earthquake Simulator Testing of Steel Plate Added Damping and Stiffness Elements," Report No. 89/02, Earthquake Engineering Research Center, University of California, Berkeley, CA.

Xia, C. and Hanson, R.D., (1992), "Influence of ADAS Element Parameters on Building Seismic Response", Journal of Structural Engineering, ASCE, Vol 118, No. 7.